Liquid Crystals

Publication details, including instructions for authors and subscription information:
http://www.informaworld.com/smpp/title~content=t713926090

Synthesis and mesomorphism of 4,4'-bis(omega-hydroxyalkoxy)-alpha-methylstilbenes

Chieh-Hao Wan; Jen-Feng Kuo; Chuh-Yung Chen

To cite this Article Wan, Chieh-Hao , Kuo, Jen-Feng and Chen, Chuh-Yung(2000) 'Synthesis and mesomorphism of 4,4'-bis(omega-hydroxyalkoxy)-alpha-methylstilbenes', Liquid Crystals, 27: 4, 523 — 532

To link to this Article: DOI: 10.1080/026782900202714

URL: http://dx.doi.org/10.1080/026782900202714

Liquid Crystals, 2000, Vol. 27, No. 4, 523–532

Synthesis and mesomorphism of 4,4′-bis(ω-hydroxyalkoxy)-α-methylstilbenes

CHIEH-HAO WAN, JEN-FENG KUO* and CHUH-YUNG CHEN
Department of Chemical Engineering, National Cheng-Kung University, Tainan, Taiwan 701, ROC

(*Received 8 December 1998; in final form 10 September 1999; accepted 9 October 1999*)

A homologous series of 4,4′-bis(ω-hydroxyalkoxy)-α-methylstilbenes, denoted HAMS-*n*, has been synthesized. Here *n* is the carbon atom length of the peripheral *n*-alkyl chain; in this work $n = 2$ to 8 and 11. The composition, microstructure, thermal properties, and mesomorphism of the homologues were determined using elemental analysis, ^{1}H NMR, FTIR, DSC, wide angle X-ray diffraction, and polarizing optical microscopy with a heating stage. The influence of the length and the even/odd numbers of methylene units of the peripheral chains on the variants of mesomorphism and the stability of mesophases, as well as on their transition temperatures, are discussed. The homologues with $n = 8$ and 11 were enantiotropic monomorphic, CrG (or CrH). The odd homologues showed monotropic trimorphism on cooling, while the even homologues exhibited enantiotropic trimorphism. A pronounced even/odd effect on the melting temperatures was observed.

1. Introduction

The study of the relationship between molecular structure and the thermotropic properties of mesogens is of fundamental interest. Whether a material exhibits a tilted mesophase or not, or has long range positional order or not, has been found to be dependent to a large degree on the nature of the functional groups, the length of the peripheral chains, and the length and breadth of the central rigid core region of the molecular structure of a smectogen.

4,4′-Dihydroxy-α-methylstilbene, constitutes an interesting mesogenic core which can be prepared in a simple and relatively inexpensive way [1–3]. Cox *et al.* [4, 5] synthesized a series of planar and non-planar *trans*-stilbene derivatives and indicated that non-planar *trans*-stilbene derivatives exhibit significantly lower melting points than their planar counterparts and assessed the role of symmetry upon the nematic clearing point. By utilizing the lower melting points and the high solubility of the α-methylstilbene derivatives, novel polymers based on 4,4′-dihydroxy-α-methylstilbene, for instance, polyesters [1, 6, 7], polyethers [8–10] and polycarbonates [11, 12], have been synthesized, and the relationships between molecular structure and the thermotropic properties reported.

Hydrogen bonding has been shown to play a role in the formation of liquid crystals and thereby influences the liquid crystalline properties [13–18]. Therefore, in this work we have synthesized a series of 4,4′-bis(ω-hydroxyalkoxy)-α-methylstilbenes which have the peripheral chains terminated with a hydroxyl group; the number of methylene units in the alkoxy groups studied were 2 to 8 and 11. The mesomorphism and thermal properties of the homologues proved to be interesting.

2. Experimental

2.1. *Characterization techniques*

Confirmation of the structures of all products was obtained by ^{1}H NMR spectroscopy (Bruker AMX 400 MHz). Elemental analysis was performed using a Heraeus CHN-O-RAPID elemental analyzer. the IR spectra were recorded (KBr disks) using a Bio-Rad, FTS-40A, FTIR spectrometer. The thermal data were recorded by differential scanning calorimetry (Du Pont 910 with RCS) at a scan rate of 5°C min^{-1} in the temperature range from 0°C to above the clearing points. The textures of the liquid crystalline phases were observed by polarizing optical microscopy—Olympus BH-2 with a LINKAM THMS 600 hot stage and a TMS 91 temperature control system. X-ray diffraction data were obtained using Ni filtered CuK$_\alpha$ radiation ($\lambda = 1.5418$ Å) with a Siemens diffractometer D5000 and a temperature controlled heating cell.

---

*Author for correspondence; e-mail: jenfkuo@mail.ncku.edu.tw

Liquid Crystals ISSN 0267-8292 print/ISSN 1366-5855 online © 2000 Taylor & Francis Ltd
http://www.tandf.co.uk/journals/tf/02678292.html

2.2. *Synthesis*

2.2.1. *4,4′-Dihydroxy-α-methylstilbene (HMS)*

HMS was synthesized by the procedure suggested by Zaheer *et al.* [2, 3]. Chloroacetone (0.3 mol) and phenol (0.6 mol) were charged into a four-necked Pyrex reactor with good stirring and kept constant at − 10°C. Concentrated H_2SO_4 (0.3 mol) was then added dropwise to the solution. The reaction was considered complete when the viscous product could no longer be stirred. The crude product was recrystallized from ethanol–water, extracted with benzene and washed with petroleum ether; m.p. 183–184°C, lit. 182–183°C, [2, 3], yield 21%.

^{1}H NMR (acetone-d_6): $\delta = 2.1$ (S, 3H, $-CH_3$), 6.6 (S, 1H, $-C{=}CH-$), 6.7 (d, 4 aromatic protons, *o* to −OH), 7.1 (d, 2 aromatic protons, *o* to α–CH_3), 7.3 (d, 2 aromatic protons, *o* to =CH), 9.4 (s, 2H, $-OH$). Found: C, 79.60; H, 6.15. Calc. for $C_{15}H_{14}O_2$: C, 79.65; H, 6.19%.

2.2.2. *4,4′-Bis(ω-hydroxyalkoxy)-α-methylstilbenes (HAMS-n)*

The HAMS-*n* homologues, except for HAMS-4, were synthesized by similar procedures. The synthesis procedure for HAMS-2 is illustrated as follows. HMS (0.06 mol), KOH (0.24 mol), and KI (0.018 mol) were charged into ethanol (150 ml). 2-Chloroethanol (0.18 mol) was added dropwise and the mixture maintained at 78°C for 36 h. The reaction mixture was then poured into water and the precipitate washed with water until it was white. An analytically pure sample was obtained by repeated recrystallization of the crude product from dioxane or ethanol, yield 81%.

^{1}H NMR (400 MHz, acetone-d_6): δ 2.22 (s, 3H), 3.87 (m, 4H, $-CH_2$–OH), 3.88 (d, 2H, $-CH_2$–OH), 4.08 (m, 4H, −Ph–O–CH_2–), 6.75 (s, 1H), 6.92–6.96 (m, 4H, aromatic protons, *o* to −OH), 7.29–7.31 (d, 2H, aromatic protons, *o* to α–CH_3), 7.46–7.49 (d, 2H, aromatic protons, *o* to =CH). FTIR (KBr): 3306, 2953, 2930, 2872, 1605, 1572, 1512, 1456, 1448, 1378, 1280, 1253, 1091, 1049, 736 cm^{-1}. Found: C, 72.55; H, 6.93. Calc. for $C_{19}H_{22}O_4$: C, 72.58; H, 7.05%.

The elementary analyses and ^{1}H NMR data for the other homologues are summarized in tables 1 and 2.

2.2.3. *4,4′-Bis(ω-hydroxybutyloxy)-α-methylstilbene*

HAMS-4 could not be obtained by the direct etherification of HMS and 4-chloro-1-butanol. The method suggested by Weissflog *et al.* [19] for the synthesis of 4,4′-bis(ω-hydroxybutyloxy)biphenyl was adopted for the preparation of HAMS-4. The synthesis was conducted under anhydrous conditions. 4,4′-Dihydroxy-α-methylstilbene (0.01 mol), 4-chlorobutyl acetate (0.022 mol), anhydrous K_2CO_3 (0.025 mol), dry acetone (35 ml), and a catalytic amount of KI were heated at reflux for 48 h. After removing the acetone KOH (0.13 mol) dissolved in ethanol/water (50 ml, 1 : 1) was added and the saponification of the acetates completed by stirring and boiling the mixture. After 7–8 h the reaction mixture was cooled to room temperature and filtered. The solid product was recrystallized from ethanol or dioxane, yield 62%.

^{1}H NMR (400 MHz, acetone-d_6); δ 1.66–1.69 (m, 4H), 1.83–1.85 (m, 4H), 2.23 (s, 3H), 3.55–3.57 (m, 2H, $-CH_2$–OH), 3.61–3.64 (m, 4H, $-CH_2$–OH), 4.04 (m, 4H, −Ph–O–CH_2–), 6.76 (s, 1H), 6.93–6.95 (m, 4H, aromatic protons, *o* to −OH), 7.30–7.33 (d, 2H, aromatic protons, *o* to α–CH_3), 7.46–7.50 (d, 2H, aromatic protons, *o* to =CH). FTIR (KBr): 3307, 2944, 2910, 2875, 1606, 1513, 1477, 1397, 1380, 1279, 1251, 1233, 1075, 1049, 1019, 745 cm^{-1}. Found: C, 74.52; H, 8.06. Calc. for $C_{23}H_{30}O_4$: C, 74.56; H, 8.16%.

2.2.4. *4-Octyloxy-4′-cyanobiphenyl (8OCB)*

4-Octyloxy-4′-cyanobiphenyl (8OCB) was prepared according to the method suggested by Goodby [20].

^{1}H NMR (400 MHz, acetone-d_6); δ 1.12–1.15 (t, 3H, $-CH_3$), 1.56–1.62 (m, 8H), 1.74 (m, 2H, −O–CH_2–CH_2–), 2.28–2.30 (m, 2H, $-CH_2$–CH_3), 4.29–4.33 (t, 2H, −Ph–O–CH_2–), 7.30–7.32 (d, 2H, aromatic protons, *o* to octyloxy), 7.92–7.95 (d, 2H,

Table 1. Yields and elemental analysis results for the 4,4′-bis(ω-hydroxyalkoxy)-α-methylstilbenes.

		Calculated/%		Found/%		
Homologue	Formula	C	H	C	H	Yield/%
HAMS-2	$C_{19}H_{22}O_4$	72.58	7.05	72.55	6.93	81
HAMS-3	$C_{21}H_{26}O_4$	73.66	7.65	73.61	7.61	75
HAMS-4	$C_{23}H_{30}O_4$	74.56	8.16	74.52	8.06	62
HAMS-5	$C_{25}H_{34}O_4$	75.34	8.60	75.30	8.68	8
HAMS-6	$C_{27}H_{38}O_4$	76.06	8.92	76.08	8.88	74
HAMS-7	$C_{29}H_{42}O_4$	76.61	9.31	76.55	9.26	50
HAMS-8	$C_{31}H_{46}O_4$	77.14	9.61	77.16	9.49	70
HAMS-11	$C_{37}H_{58}O_4$	78.40	10.31	78.37	10.25	61

Table 2. ^{1}H NMR chemical shifts obtained at room temperature for the HAMS-*n* homologues.

Homologue	^{1}H NMR (400 MHz, ppm)
HAMS-2	(Acetone-d_6); δ 2.22 (s, 3H), 3.87 (m, 4H, $-\mathrm{C}\mathit{H}_2-\mathrm{OH}$), 3.88 (d, 2H, $-\mathrm{CH}_2-\mathrm{O}\mathit{H}$), 4.08 (m, 4H, $-\mathrm{Ph}-\mathrm{O}-\mathit{CH}_2-$), 6.75 (s, 1H), 6.92–6.96 (m, 4H, aromatic protons, *o* to $-\mathrm{OH}$), 7.29–7.31 (d, 2H, aromatic protons, *o* to $\alpha-\mathrm{CH}_3$), 7.46–7.49 (d, 2H, aromatic protons, *o* to $=\mathrm{CH}$).
HAMS-3	(Acetone-d_6); δ 1.97 (m, 4H), 2.23 (s, 3H), 3.63 (t, 2H, $-\mathrm{O}\mathit{H}$), 3.73 (m, 4H), 4.13 (t, 4H, $-\mathrm{Ph}-\mathrm{O}\mathit{CH}_2-$), 6.76 (s, 1H), 6.92–6.97 (m, 4H, aromatic protons, *o* to $-\mathrm{OH}$), 7.29–7.33 (d, 2H, aromatic protons, *o* to $\alpha-\mathrm{CH}_3$), 7.46–7.49 (d, 2H, aromatic protons, *o* to $=\mathrm{CH}$).
HAMS-4	(Acetone-d_6); δ 1.66–1.69 (m, 4H), 1.83–1.85 (m, 4H), 2.23 (s, 3H), 3.55–3.57 (m, 2H, $-\mathrm{CH}_2-\mathrm{O}\mathit{H}$), 3.61–3.64 (m, 4H, $-\mathrm{C}\mathit{H}_2-\mathrm{OH}$), 4.04 (m, 4H, $-\mathrm{Ph}-\mathrm{O}-\mathit{CH}_2-$), 6.76 (s, 1H), 6.93–6.95 (m, 4H, aromatic protons, *o* to $-\mathrm{OH}$), 7.30–7.33 (d, 2H, aromatic protons, *o* to $\alpha-\mathrm{CH}_3$), 7.46–7.50 (d, 2H, aromatic protons, *o* to $=\mathrm{CH}$).
HAMS-5	(Acetone-d_6); δ 1.57 (m, 8H), 1.79 (m, 4H), 2.22 (m, 3H), 3.36 (t, 2H, $-\mathrm{O}\mathit{H}$), 3.56 (m, 4H), 4.01 (t, 4H, $-\mathrm{Ph}-\mathrm{O}\mathit{CH}_2-$), 6.74 (s, 1H), 6.92 (m, 4H, aromatic protons, *o* to $-\mathrm{OH}$), 7.29–7.31 (d, 2H, aromatic protons, *o* to $\alpha-\mathrm{CH}_3$), 7.45–7.47 (d, 2H, aromatic protons, *o* to $=\mathrm{CH}$).
HAMS-6	(Acetone-d_6); δ 1.41–1.56 (m, 12H), 1.75–1.81 (m, 4H), 2.22 (s, 3H), 3.31 (t, 2H, $-\mathrm{CH}_2-\mathrm{O}\mathit{H}$), 3.52–3.57 (m, 4H, $-\mathit{CH}_2-\mathrm{OH}$), 4.01 (t, 4H, $-\mathrm{Ph}-\mathrm{O}-\mathrm{C}\mathit{H}_2-$), 6.74 (s, 1H), 6.90–6.94 (m, 4H, aromatic protons, *o* to $-\mathrm{OH}$), 7.29–7.31 (d, 2H, aromatic protons, *o* to $\alpha-\mathrm{CH}_3$), 7.45–7.47 (d, 2H, aromatic protons, *o* to $=\mathrm{CH}$).
HAMS-7	(DMSO-d_6); δ 1.33 (m, 16H), 1.69 (m, 4H), 2.16 (m, 3H), 3.40 (m, 4H), 3.95 (t, 4H, $-\mathrm{Ph}-\mathrm{O}-\mathit{CH}_2-$), 4.35 (t, 2H, $-\mathrm{O}\mathit{H}$), 6.73 (s, 1H), 6.92 (m, 4H, aromatic protons, *o* to $-\mathrm{OH}$), 7.26–7.30 (d, 2H, aromatic protons, *o* to $\alpha-\mathrm{CH}_3$), 7.43–7.47 (d, 2H, aromatic protons, *o* to $=\mathrm{CH}$).
HAMS-8	(DMSO-d_6); δ 1.23–1.42 (m, 20H), 1.67–1.74 (m, 4H), 2.17 (s, 3H), 3.36–3.41 (m, 4H, $-\mathrm{C}\mathit{H}_2-\mathrm{OH}$), 3.95–3.98 (t, 4H, $-\mathrm{Ph}-\mathrm{O}-\mathrm{C}\mathit{H}_2-$), 4.12–4.15 (t, 2H, $-\mathrm{CH}_2-\mathrm{O}\mathit{H}$), 6.71 (s, 1H), 6.88–6.92 (m, 4H, aromatic protons, *o* to $-\mathrm{OH}$), 7.26–7.28 (d, 2H, aromatic protons, *o* to $\alpha-\mathrm{CH}_3$), 7.42–7.44 (d, 2H, aromatic protons, *o* to $=\mathrm{CH}$).
HAMS-11	(DMSO-d_6); δ 1.27–1.46 (m, 32H), 1.71 (m, 4H), 2.17 (s, 3H), 3.39 (m, 4H), 3.98 (m, 4H, $-\mathrm{Ph}-\mathrm{O}-\mathit{CH}_2-$), 4.01 (t, 2H, $-\mathrm{O}\mathit{H}$), 6.70 (s, 1H), 6.90 (m, 4H, aromatic protons, *o* to $-\mathrm{OH}$), 7.26–7.28 (d, 2H, aromatic protons, *o* to $\alpha-\mathrm{CH3}$), 7.42–7.44 (d, 2H, aromatic protons, *o* to $=\mathrm{CH}$).

aromatic protons, *o* to $-\mathrm{CN}$), 8.06–8.07 (m, 4H, aromatic protons, *m* to $-\mathrm{CN}$ and *m* to octyloxy). FTIR (KBR): 2956, 2935, 2921, 2854, 2232, 1605, 1579, 1521, 1496, 1393, 1289, 1265, 1252, 1031, 815, 722 cm^{-1}. Found: C, 81.89; H, 8.21; N, 4.52. Calc. for $\mathrm{C}_{21}\mathrm{H}_{25}\mathrm{NO}$: C, 82.04; H, 8.20; N, 4.56%.

The product is a well known reference material and had the following transition temperatures in agreement with the literature: Cr–54°C–SmA–67°C–N–80°C–I (lit. Cr–54°C–SmA–67°C–N–80°C–I, [21]).

2.2.5. *4,4′-Bis(6-hydroxyhexyloxy)biphenyl (BHHBP)*

The synthesis of 4,4′-bis(6-hydroxyhexyloxy)biphenyl (BHHBP) has been described in detail elsewhere [22, 23]. Briefly, 4,4′-dihydroxybiphenyl was suspended in an excess of ethanolic NaOH with a small amount of KI, and 6-chlorohexan-1-ol was added dropwise. The mixture was heated at reflux overnight, and the required product was separated and purified by recrystallization from *n*-butanol or *n*-butanol/dioxan mixtures, yield 45%. The product had the phase transition temperatures: Cr–97°C–CrG (or CrH)–173°C–I (lit. Cr–98°C–CrG (or CrH)–179°C–I, [24]). Found: C, 74.48; H, 8.76. Calc. for $\mathrm{C}_{24}\mathrm{H}_{34}\mathrm{O}_4$: C, 74.58; H, 8.86%.

3. Results and discussion

The 4,4′-bis(ω-hydroxyalkoxy)-α-methylstilbene series is denoted HAMS-*n*, where *n* = 2, 3, 4, 5, 6, 7, 8 and 11. The general synthetic route, except for HAMS-4 (see above), is summarized as follows:

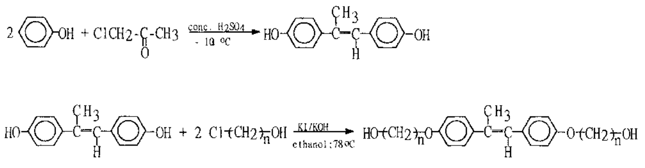

The procedure for synthesis of the mesogenic diol 4,4′-dihydroxy-α-methylstilbene follows the work of Zaheer *et al.* [2], which gave the *trans*-isomer. Accordingly, the molecular lengths of the HAMS-*n* homologues (table 3) are estimated based on the assumption of the *trans*-configuration of the α-methyl stilbene moiety and an extended zig-zag conformation of the peripheral alkyl chains.

Table 3. Experimental and predicted[a] *d*-spacings of the smectic layers of the HAMS-*n* homologues. Parentheses indicate the value at room temperature.

Homologue	$2\theta^{b}$/°	Found/Å	Calculated*/Å
HAMS-2	4.69	18.84^{c}	20.88
HAMS-3	4.13 (4.34)	21.39^{c} (20.34)	23.50
HAMS-4	3.84 (4.14)	23.02^{c} (21.33)	25.81
HAMS-5	3.42 (4.00)	25.90^{c} (22.06)	28.62
HAMS-6	3.27 (3.55)	27.00^{c} (24.88)	30.73
HAMS-7	3.32 (3.52)	26.60^{c} (25.10)	33.72
HAMS-8	2.73 (2.78	32.30^{c} 31.76^{d}	36.05
HAMS-11	2.14 (2.28)	41.20^{c} (38.80)	42.25

[a] Predicted values based on the *trans*-α-methylstilbene configuration and extended alkyl chain model using the CERIUS^{2} software with Dreiding force field.

[b] 2θ X-ray diffraction angle.

[c] Value obtained at the temperature showing a mosaic texture.

[d] Value obtained at 40°C.

3.1. *DSC analysis*

Typical DSC heating and cooling traces recorded at a rate of 5°C min^{-1} are shown in figures 1 and 2. The odd homologues, HAMS-3, 5, and 7, showed one exotheric peak on heating and two endothermic peaks on cooling. The width of the two exothermic peaks is not large, and the peaks overlap only for HAMS-7. However, the even homologues HAMS-4 and 6, both give three separated endotherms on heating and three exotherms, whereas HAMS-2 has only two exotherms, without involving any supercooling. HAMS-11 and HAMS-8 exhibit two well separated endotherms and exotherms on both heating and cooling. Below we will show that all the homologues exhibited certain mesophase textures. Accordingly, HAMS-11 and HAMS-8 are enantiotropic monomorphic mesogens. The odd homologues ($n = 3$, 5 and 7) seem to be monotropic dimorphic mesogens. The even homologues ($n = 2$, 4 and 6) may be enantiotropic dimorphic mesogens. The thermal transitions and thermodynamic properties associated with the various traces are summarized in table 4. In the table, the temperatures for the transitions of isotropization to the nematic phase and of the CrG (or CrH) phase to the crystalline phase, which could not be detected by DSC, were determined by POM measurements (giving higher values when they can be compared with DSC values).

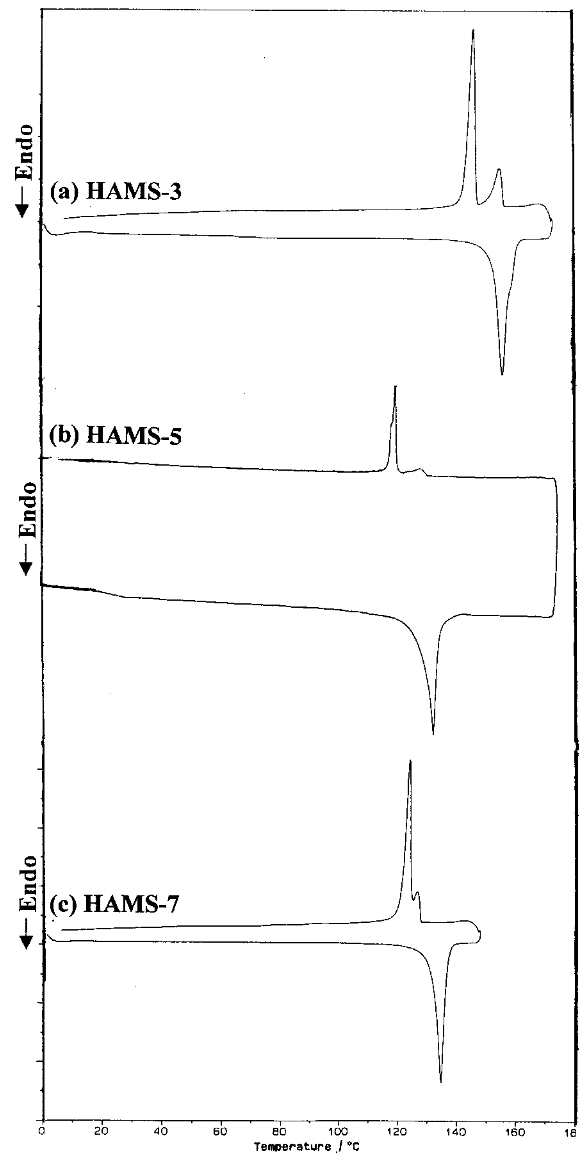

Figure 1. DSC thermograms of three HAMS-*n*: (*a*) HAMS-3, (*b*) HAMS-5, (*c*) HAMS-7.

Figure 3 shows the melting points (T_{m}), and the isotropization temperatures (T_{i}) as a function of length of the alkyl peripheral chains of the homologues. The two transition temperatures decreased with increasing length of the peripheral alkyl chains. A very significant even-odd effect was shown by the melting temperatures, but not for the isotropization temperatures.

From table 4, the value of the entropy change for HAMS-11 on melting is only about 7 J mol^{-1} K^{-1}, which is about one third that for HAMS-8. On the contrary, the value of the entropy change for the

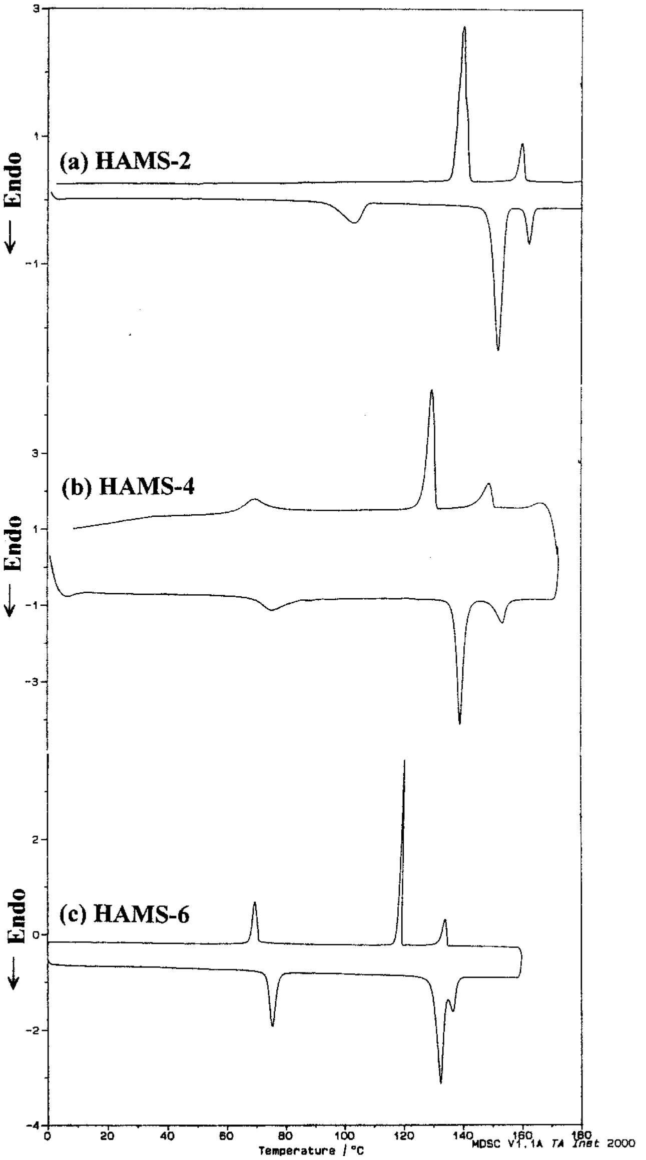

Figure 2. DSC thermograms of three HAMS-*n*: (*a*) HAMS-2, (*b*) HAMS-4, (*c*) HAMS-6.

transition of the mesophase to the isotropic phase is about 210 J mol^{-1} K^{-1}, which is about twice that for HAMS-8. For both homologues, the entropy change for the transition of the mesophase (a soft crystal) to the isotropic phase is significantly greater than that for melting. For the other homologues, the largest entropy change is for the transition of the CrG (or CrH) phase to SmA, and the smallest is for the transition of the SmA to the nematic phase. Among the homologues studied, HAMS-7 has the largest entropy change for the transition from CrG (or CrH) phase to SmA. HAMS-5 has the smallest entropy change for the transition of the SmA phase to the nematic phase.

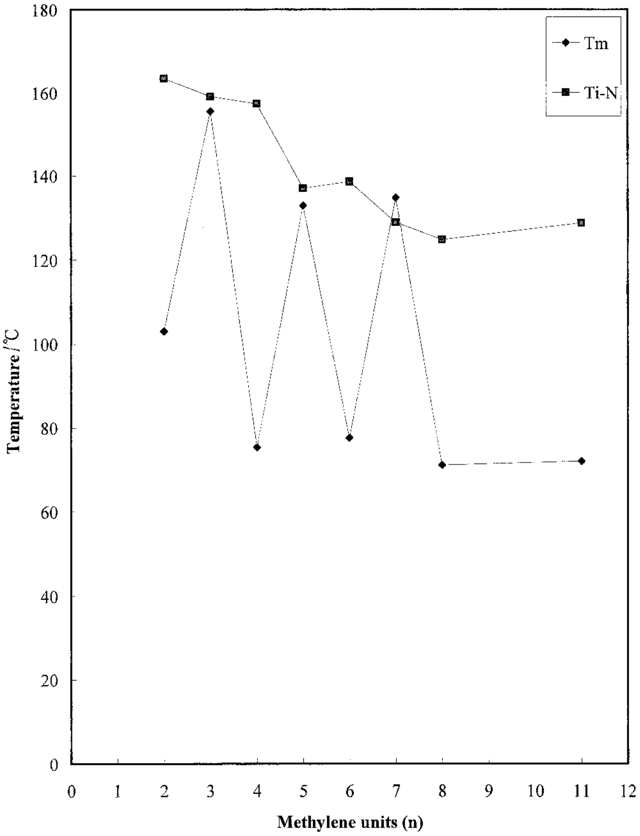

Figure 3. Phase transition temperatures vs. the number of methylene units (*n*) of the peripheral chains of the HAMS-*n* homologues.

3.2. *POM textures and wide angle X-ray diffractograms*

The textures of liquid crystalline mesophases and the rule of phase sequences can be used to obtain a first estimate of mesophase types [25–27]. In the present study, we attempted to elucidate the mesophase types of the homologues by observing the textures by polarizing optical microscopy (POM), coupled with determinations of the patterns of the wide angle X-ray (WAXR) diffractograms, and/or appropriate miscibility studies [28, 29]. The conclusions have already been used in table 4 to summarize the results for the mesophase types, the variants of mesomorphism and the transition temperature for the mesophases.

3.2.1. *The mesophase of HAMS-8 and 11*

HAMS-8 and 11 give similar mesophase textures and wide angle X-ray diffraction patterns, as illustrated here for HAMS-8. From POM, HAMS-8 gave a transition from isotropic to a mosaic texture at 125°C, followed by a transition to a mosaic texture superimposed with clear striations at 68°C. These textures were closely similar to the mosaic texture and the mosaic texture with

Table 4. Phase transition temperatures (T/°C) and entropy changes (ΔS/J mol^{-1} K^{-1}) for the HAMS-*n* homologues, obtained mainly by DSC: HO–(CH$_2$)$_n$–O–C$_6$H$_4$–C(CH$_3$)=CH–C$_6$H$_4$–O–(CH$_2$)$_n$–OH. Parentheses indicate the values for monotropic phase transitions observed during cooling processes.

Homologue	Formula		Cr	•	CrG or CrH	•	SmA	•	N	•	I
HAMS-2	$C_{19}H_{22}O_4$	H^{b}	•	103.0/27.5	•	149.3/52.9	•	160.4^{c}/10.8	•	165.0^{a}	•
		C	•	75^{a}/—	•	136.4/64.0	•	156.7/11.1	•	164.5^{a}	•
HAMS-3	$C_{21}H_{26}O_4$	H	•							155.5/74.9	•
		C	•	(80.0/—)^{a}	•	(144.0/60.2)	•	(153.3/15.1)	•	159.1^{a}	•
HAMS-4	$C_{23}H_{30}O_4$	H	•	75.3/16.7	•	139.2/50.2	•	153.4/12.2	•	159.2^{a}	•
		C	•	69.5/16.5	•	129.5/52.7	•	148.8/12.8	•	157.3^{a}	•
HAMS-5	$C_{25}H_{34}O_4$	H	•							132.9/69.0	•
		C	•	(70.0/—)^{a}	•	(117.7/55.7)	•	(127.6/7.6)	•	137.0^{a}	•
HAMS-6	$C_{27}H_{38}O_4$	H	•	77.6/49.7	•	133.3/82.0	•	137.8/20.8	•	140.5^{a}	•
		C	•	71.7/45.9	•	121.9/97.2	•	135.0/22.6	•	138.6^{a}	•
HAMS-7	$C_{29}H_{42}O_4$	H	•							134.8/113.9	•
		C	•	(55.0/—)^{a}	•	(124.0/102.2)	•	(126.9/8.6)	•	128.9^{a}	•
HAMS-8	$C_{31}H_{46}O_4$	H	•	76.8/24.2	•					133.8/104.1	•
		C	•	68.4/25.8	•					125.0/104.1	•
HAMS-11	$C_{37}H_{58}O_4$	H	•	72.0/7.1	•					137.0/209.7	•
		C	•	68.5/8.1	•					128.8/215.5	•

[a] Phase transition temperatures determined by POM.
[b] H: heating process; C: cooling process.
[c] From [31] the isotropization temperature of the compound is given as 160°C.

striations (fracture pattern), respectively of HAMS-6 (see next section). On heating, the textures appeared in the reverse order at higher temperatures. The possible smectic phases with a mosaic texture are SmB, CrE, SmF, SmI, and CrG (or CrH) [25, 26].

Figure 4 shows the WAXR diffraction patterns of HAMS-8 at 100°C and 40°C on cooling. The spectrum at 40°C presents quite a strong diffraction peak at $2\theta = 2.78°$ and several diffraction peaks in the region of long range positional order. At 100°C the spectrum did not essentially change, except that the peak widths broadened and the *d*-spacing of the diffraction peaks increased. The *d*-spacing at 100°C corresponding to $2\theta = 2.73°$ is about 32.3 Å which is shorter than the calculated value based on the molecular length with a zig-zag extended chain (36.05 Å, table 3), indicating that the constituent molecules are tilted with respect to the mesophase layer planes. Thus, the phase with the mosaic texture and a tilted layer structure may be assumed to be crystal G phase (CrG) or CrH. For miscibility studies, 4,4′-bis(6-hydroxyhexyloxy)biphenyl (BHHBP), which shows the CrG (or CrH) phase [24] was synthesized and used as the standard.

Figure 5 shows the phase diagram for the full composition range of binary mixtures of HAMS-8 and BHHBP. The system obviously obeys the rule of miscibility and shows that the mesophase of HAMS-8 with the mosaic texture is a CrG (or CrH) phase. The

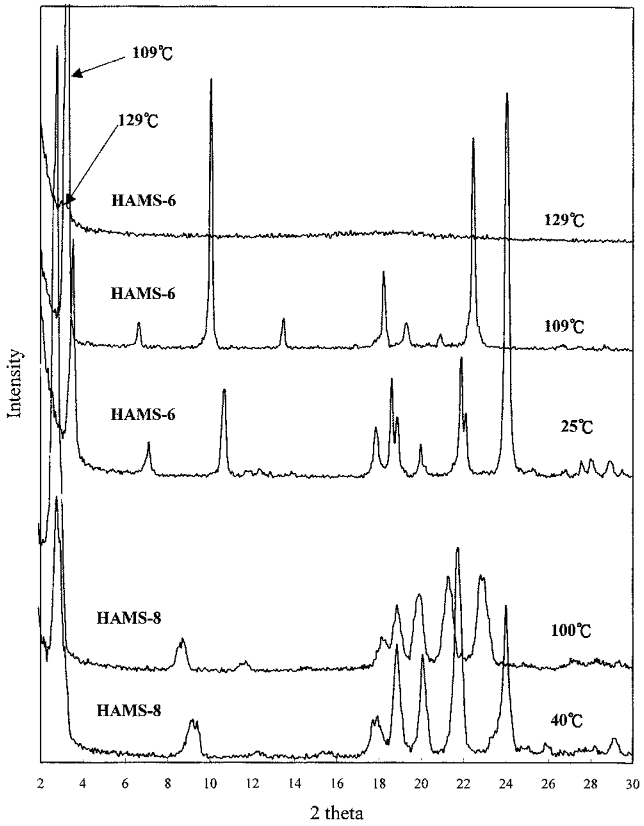

Figure 4. X-ray diffraction patterns of HAMS-8 and HAMS-6 at the indicated temperatures.

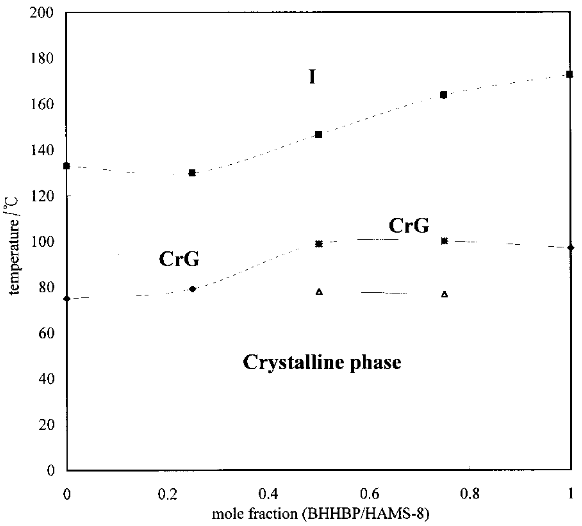

Figure 5. Binary phase diagram of HAMS-8 and 4,4′-bis-(6-hydroxyhexyloxy)biphenyl (based on heating traces).

phase showing the fracture pattern is of course a crystalline phase. Consequently, HAMS-8 is enantiotropic monomorphic with the sequence I–125°C–CrG (or CrH–68°C–Cr) (on cooling).

3.2.2. *The mesophases of the even numbered homologues with n = 2 to 6*

The even numbered homologues all exhibited similar textures and X-ray diffraction patterns. HAMS-6 is taken as an illustration. According to DSC, as mentioned above, HAMS-6 appears to be an enantiotropic dimorphic mesogen. POM revealed a texture of droplets with crosses at *c.* 139°C, and as shown in figure 6, a focal-conic fan-like texture at 130°C, a mosaic texture at 115°C, and a texture with a fracture pattern at below 72°C. Heating gave the same textures in reverse order. Obviously, HAMS-6 is polymorphic. Therefore, the DSC measurements did not detect all the mesophase transitions. As is well known [26, 27], the droplets with crosses are characteristic of a nematic (N) phase, the focal-conic fan-like texture is characteristic of a smectic A (SmA) phase, and the mosaic texture could be characteristic of the smectic phases mentioned for HAMS-8 and 11.

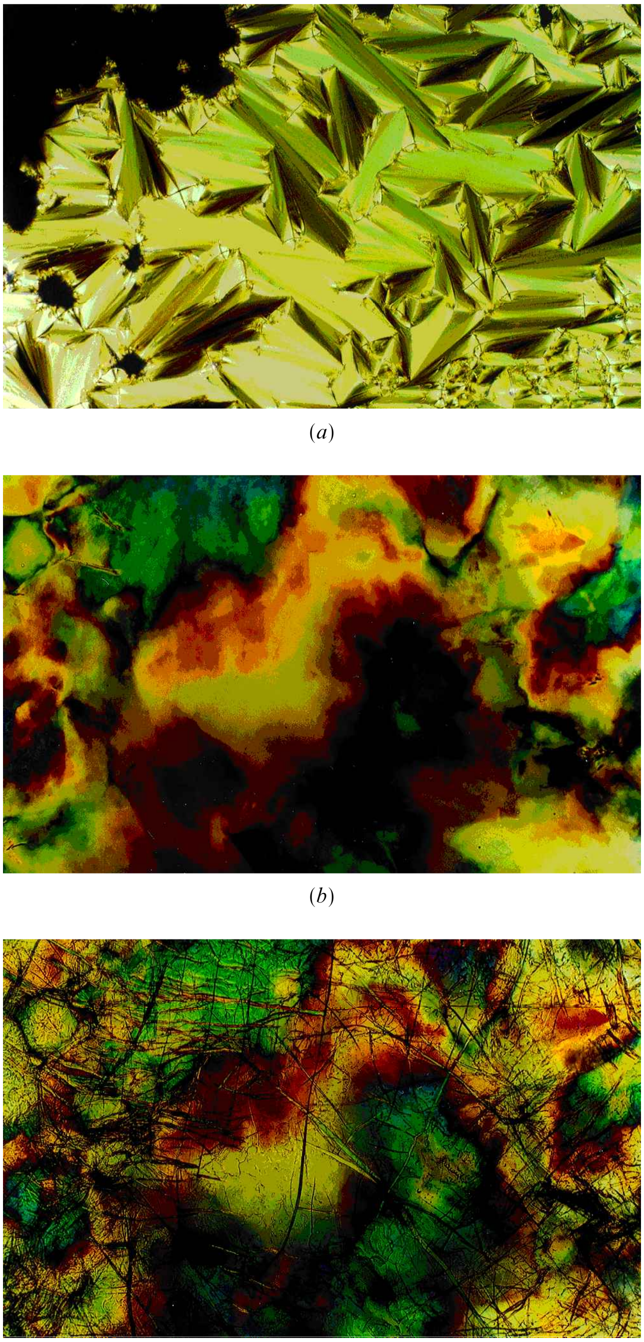
(*a*)

(*b*)

(*c*)

Figure 6. Textures of HAMS-6 observed between crossed polarizers on cooling to the indicated temperatures. (*a*) 130°C (× 120) focal-conic texture; (*b*) 115°C (× 120) mosaic texture; (*c*) 32°C (× 120) mosaic texture with superimposed fine striations.

Figure 4 presents the WAXR diffraction patterns of HAMS-6 at various temperatures on cooling. The diffraction spectrum above 135°C was typical of an amorphous system. The spectrum at temperatures between 135 and 122°C showed distinct diffraction at $2\theta = 3.05°$ and a diffuse peak in the region of long range positional order. The *d*-spacing corresponding to $2\theta = 3.05°$ is 28.9 Å, which is again shorter than the molecular length calculated for a zig-zag extended chain model (30.7 Å), indicating that the smectic phase might have a tilted arrangement of the constituent molecules, which is not in agreement with the SmA assignment suggested by the POM texture. In the temperature range 122 and 72°C, the spectrum presents quite strong diffraction at $2\theta = 3.27°$, several peaks in the long range order region ($2\theta = 18°$ to 22.8°), as well as several interlayer diffractions at $2\theta = 6.5°$ to 14°. The *d*-spacing corresponding to $2\theta = 3.27°$ is 27.0 Å, which is once more shorter than the molecular length calculated on a zig-zag extended chain model (30.7 Å). Overall, these results indicate that the smectic phase has a pseudo three-dimensional order with tilted constituent molecules. Thus, the mesophase with the mosaic texture is consistent with a CrG (or CrH) phase. The spectrum at 25°C is typical of a crystalline solid.

A miscibility study was performed to solve the ambiguous nature of the mesophase type in the temperature range 122 to 135°C. 8OCB is known to have the phase sequence Cr–54°C–SmA–67°C–N–80°C–I [21]; this was synthesized and used as a standard for the miscibility study. The phase diagram shown in figure 7 indicates that the smectic mesophase of HAMS-6 can be marked with the same symbol as that of 8OCB. The mesophase is thus assigned as a SmA phase. Consequently, the variants of the trimorphism of HAMS-6 are proposed as I–138.6°C–N–135°C–SmA–122°C–CrG (or CrH)–72°C–Cr (based on cooling), which is in agreement with the phase sequence rule [26]. The fact that the SmA phase has thinner layers may be attributed to the liquid-like nature of the end chains and/or chain fluidity and intermixing [30].

3.2.3. *The mesophases of the odd number homologues with n = 3 to 7*

As mentioned, the cooling DSC spectra indicate that HAMS-7, 5 and 3 might probably all be monomorphic mesogens. However, POM measurements revealed that they are trimorphic mesogens because they all exhibited four kinds of texture on cooling, which are similar to those of HAMS-6. According to wide angle X-ray diffraction, miscibility and the rule of phase sequence, the monotropic trimorphism of these odd numbered homologues was assigned as N, SmA, and CrG (or CrH).

It is noteworthy that the thermal stability of the liquid crystal phases varies greatly with the length of the peripheral chains. From the DSC (table 3), HAMS-7 gave two overlapped exothermic peaks and the temperature range of the nematic phase and the SmA phase was only 2°C. It is interesting to study the POM textures of HAMS-7 at 126 and 125°C during cooling. As shown in figure 8, the nematic droplets and the bâtonnet texture in the isotropic melt simultaneously coexisted at 126°C, and the focal-conic texture and the grandular pattern (CrG or CrH) coexisted at 125°C. The results imply that HAMS-7 coexists as three phases at 126°C and as two phases at 125°C. This coexistence of multiple phases is of course related to the narrow temperature ranges of the phases. Despite measuring the wide angle X-ray diffraction patterns in the temperature range 126 to 124°C many times, the patterns obtained were always

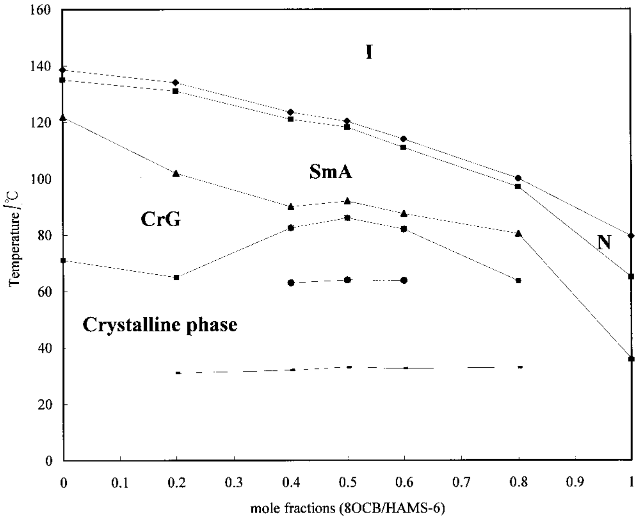

Figure 7. Binary phase diagram of HAMS-6 and 4-octyloxy-4′-cyanobiphenyl (based on the cooling traces).

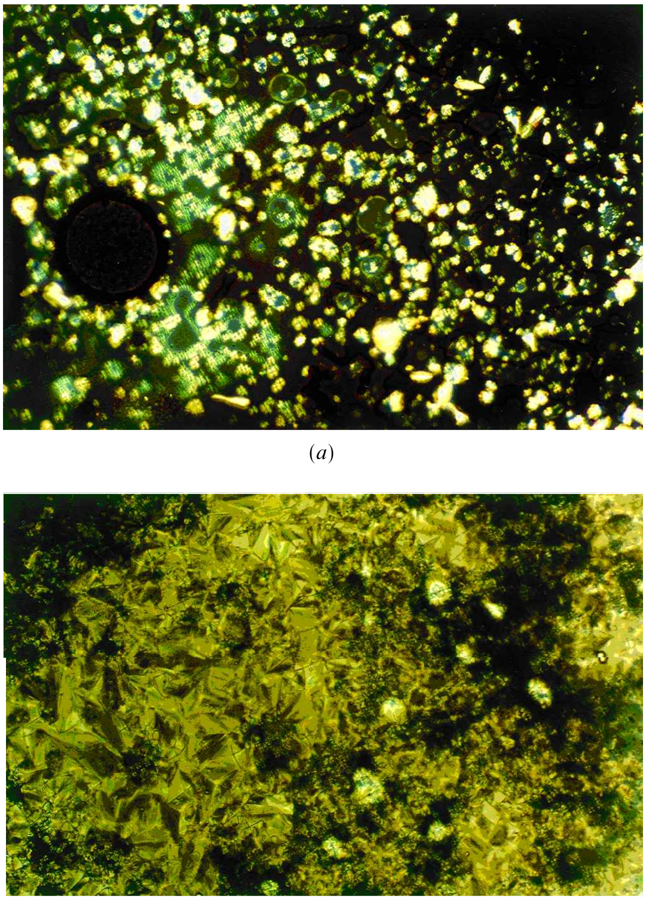
(*a*)

(*b*)

Figure 8. Textures of HAMS-7 observed between crossed polarizers on cooling from isotropic liquid (×120): (*a*) 126°C, (*b*) 125°C.

similar to that obtained at 124°C (CrG or CrH) rather than that of a SmA phase. Again this is caused by the transitions of the consecutive mesophases occurring very close together, and the coexistence of multiple phases.

3.3. *Comparison between the methyl terminal trans-α-methylstilbenes and 4,4′-bis(hydroxyhexyloxy)biphenyl*

Cox and coworkers [4, 5] synthesized a series of *trans*-4,4′-dialkoxy-α-methylstilbenes (AMS-*n*, $n \leqq 8$), and showed that they had nematic phases with lower transition temperatures than the parent stilbenes. The HAMS-*n* compounds with the peripheral chain corresponding to AMS-*n*, that is, $n = 2$ to 6, exhibited nematic, SmA and CrG (or CrH) phases with higher transition temperatures. Obviously, HAMS-2 to HAMS-6 have more ordered mesophases than the AMS-*n* homologues. The difference between the HAMS-*n* and AMS-*n* series is only in the terminal group of the peripheral chain, one having a terminal polar hydroxyl group and the other a non-polar methyl group. Therefore, the terminal OH group that could give hydrogen bonding effects might play an important role for obtaining smectic phases and higher transition temperatures.

MacKnight *et al.* [24] reported that 4,4′-bis(hydroxyhexyloxy)biphenyl (BHHBP) exhibited monomorphism, namely CrG (or CrH). HAMS-6, which has the same peripheral chain length as BHHBP, however, is enantiotropic trimorphic involving nematic, SmA and CrG (or CrH) phases. It is also revealed that the liquid crystal phases of HAMS-6 are not as thermally stable as that of BHHBP. It is noteworthy that HAMS-8 and 11 are enantiotropic monomorphic with a CrG (or CrH) phase, similarly to BHHBP. Therefore, the homologues of HAMS-*n* require a longer peripheral chain to give a single CrG (or CrH) phase. It may be that the more complicated geometric molecular structure of the α-methylstilbenes, with a bulky methyl substituent, is responsible for this difference.

4. Conclusions

The length of the peripheral ω-hydroxyalkyl chain profoundly influences the mesomorphic properties of the compounds studied. The even numbered homologues all show enantiotropic mesomorphism, while the odd numbered homologues exhibit monotropic mesomorphisms except for the homologue with $n = 11$. HAMS-8 and 11 are monomorphic with a CrG (or CrH) phase, while the homologues with $n < 8$ are trimorphic. The narrow ranges of the SmA and N phases of HAMS-7 resulted in the coexistence of multiple phases consisting of the isotropic melt, the nematic phase and the SmA phase. The transition from isotropic liquid to the nematic phase could not be detected by DSC, but could be observed by POM.

The authors are indebted to the National Science Council of the Republic of China for financial support of this work (NSC-87-2216-E-006-007). The authors wished to thank Professor Stephen Cheng, Institute of Polymer Science, The University of Arkon, Ohio, USA, for his useful suggestion of this study. Mr Chen Cai-Yau is also thanked for his kindness in helping with the purification of the compounds.

References

[1] Roviello, A., and Sirigu, A., 1980, *Makromol. Chem.*, **181,** 1799.

[2] Zaheer, S. H., and Bhushan, B., 1953, *Nature*, **171,** 746.

[3] Zaheer, S. H., Singh, B., Bhushan, B., Bhargava, P. M., Kacker, I. K., Ramachandran, K., Sastri, V. D., and Rao, N. S., 1954, *J. chem. Soc.*, 3360.

[4] Cox, R. J., Young, W. R., and Aviram, A., 1972, *J. Am. chem. Soc.*, **94,** 3976.

[5] Cox, R. J., 1972, *Mol. Cryst. liq. Cryst.*, **19,** 111.

[6] Roviello, A., and Sirigu, A., 1982, *Makromol. Chem.*, **183,** 409.

[7] Roviello, A., and Sirigu, A., 1982, *Makromol. Chem.*, **183,** 895.

[8] Percec, V., Shaffer, T. D., and Nava, H., 1984, *J. Polym. Sci. polym. Lett.*, **2,** 637.

[9] Percec, V., Asami, K., and Tomazos, D., 1991, *Mol. Cryst. liq. Cryst.*, **205,** 47.

[10] Percec, V., Asami, K., and Tomazos, D., 1991, *Mol. Cryst. liq. Cryst.*, **205,** 67.

[11] Cebe, P., Carbeck, J., Schreuder-Libson, H., Bluhm, A., and Yeomans, W., 1992, *Polym. Preprints*, **33,** 331.

[12] Cheng, Y. Y., Cebe, P. *et al.*, 1994, *Macromolecules*, **87,** 5440.

[13] Jeffrey, G. A., 1986, *Acc. chem. Res.*, **19,** 168.

[14] Kato, T., and Frechet, J. M. J., 1990, *Macromolecules*, **23,** 360.

[15] Kato, T., and Frechet, J. M. J., 1989, *J. Am. chem. Soc.*, **111,** 8533.

[16] Kato, T., Adachi, H., Fujishima, A., and Frechet, J. M. J., 1992, *Chem. Lett.*, 256.

[17] Tschierske, C., Brezesinski, G., Kuschel, F., and Zaschke, H., 1989, *Mol. Cryst. liq. Cryst.*, **6,** 139.

[18] Li, M., Qui, H. J., Chen, X. F., Li, G., and Zhou, E. L., 1999, *Liq. Cryst.*, **26,** 1053.

[19] Rotz, U., Lindau, J., Weissflog, W., Reinhold, G., Unseld, W., and Kuschel, F., 1989, *Mol. Cryst. liq. Cryst.*, **170,** 185.

[20] Goodby, J. W., 1998, in *Handbook of Liquid Crystals*, Vol. 2A, edited by D. Demus, J. W. Goodby, G. W. Gray, H.-W. Spiess, and V. Vill (Weinheim: Wiley-VCH), p. 426.

[21] Pugh, C., and Kriste, A. L., 1998, in *Handbook of Liquid Crystals*, Vol. 3, edited by D. Demus, J. W. Goodby, G. W. Gray, H.-W. Spiess, and V. Vill (Weinheim: Wiley-VCH), p. 156.

[22] Reck, B., and Ringsdorf, H., 1985, *Makromolek. Chem. rapid Commun.*, **6,** 291 and 691.

[23] Stenhouse, P. J., Valles, E. M., MacKnight, W. J., and Kantor, S. W., 1989, *Macromolecules*, **22,** 1467.

[24] Smyth, G., Pollack, S. K., MacKnight, W. J., and Hsu, S. L., 1990, *Liq. Cryst.*, **7,** 839.

[25] Keller, H., and Hatz, R., 1980, in *Handbook of Liquid Crystals* (Weinheim: Verlag Chemie), pp. 1–29.

[26] Demus, D., Diele, S., Grande, S., and Sackmann, H., 1983, in *Advances in Liquid Crystals*, edited by G. H. Brown (New York: Academic Press), pp. 1–85.

[27] Demus, D., and Richter, L., 1978, in *Textures of Liquid Crystals* (Weinheim: Verlag Chemie), pp. 100–101.

[28] Sackmann, H., and Demus, D., 1966, *Mol. Cryst. liq. Cryst.*, **2,** 81.

[29] Sackmann, H., and Demus, D., 1973, *Mol. Cryst. liq. Cryst.*, **21,** 239.

[30] Private communication from Professor G. W. Gray.

[31] Seiber, R. H., 1969, *Liebigs Ann. Chem.*, **730,** 31.